Chaotic Systems that are Robust to Added Noise

05.45.Vx, 05.45.Gg, 87.10.+e

Thomas L. Carroll
US Naval Research Lab

While added noise can destroy synchronization in synchronized chaotic systems, it was shown that some chaotic systems were not sensitive to added noise. In this paper, the mechanism for this noise resistance is explored. It is seen that part of the chaotic system acts like it is resonant, reducing the noise sensitivity of the system. By comparing to a model of a neuron, it is speculated that similar mechanisms may also be present in biological systems.

Many chaotic systems may be synchronized by sending a signal from a drive chaotic system to a response chaotic system. It has been suggested that this type of synchronization might be useful as a form of spread spectrum communications, where using a carrier signal with a broad frequency spectrum allows one to transmit more information in a given frequency band. One problem with this application of synchronized chaos is that any signal that is transmitted inevitably picks up additive noise, and many chaotic response systems are very sensitive to this added noise. One type of chaotic system has been demonstrated that is not as sensitive to added noise. This type of chaotic system consists of a fast part coupled to a slow part. While it has been shown that increasing the time scale separation between fast and slow parts increases the ability of these systems to resist added noise, no reason for this noise resistance was given. In this paper, I apply mathematical approximation techniques that allow me to look at the slow part of the

chaotic system by itself, and I see some characteristics of the slow dynamics that are associated with noise resistance (also called noise robustness).

Introduction

When chaos synchronization was first described [1], it appeared that it would be useful for spread spectrum communications [2-9], since chaotic signals are naturally broad band. Unfortunately, most synchronized chaotic response systems that were studied were very sensitive to noise added to the synchronizing signal. [10, 11] As little as 10% noise added to the driving signal could destroy all evidence of synchronization.

It was later shown that not all synchronizing chaotic systems were so sensitive to added noise, and in some cases added noise could even enhance chaotic synchronization [12-15]. A review of some of the more general types of chaotic synchronization and the effects of noise on synchronization may be found in [16].

In this paper I am interested in some chaotic systems that were shown to be not very sensitive to added noise [17, 18]. These particular systems consisted of a Rossler-like chaotic system coupled to a nonlinear oscillator with a much lower frequency. Synchronization could be confirmed in these systems even when the added noise amplitude was much larger than the driving signal. The greater the frequency difference between the faster and slower parts of these chaotic systems, the more robust the synchronization was to noise.

While these chaotic systems were easy to describe, the reason that they were robust to added noise was never determined. In this paper, I examine the original noise robust chaotic system as a function of a parameter which can make the system noise

robust or non noise robust. I describe the difference between noise robust and non noise robust states for the chaotic system.

Noise Robust System

The 2-frequency Rossler chaotic system is described by [17, 18]

$$\begin{aligned}
\frac{dx_1}{dt} &= -\left(\gamma_{11}x_1 + \gamma_{12}x_2 + x_3 + \beta x_4\right) \\
\frac{dx_2}{dt} &= -\left(x_1 - \gamma_{22}x_2\right) \\
\frac{dx_3}{dt} &= -\left(g\left(x_1\right) + x_3\right) \\
\frac{dx_4}{dt} &= -\alpha\left(\gamma_{44}x_4 + \gamma_{45}x_5 + x_6 + \gamma_{41}\left|x_1\right|\right) \\
\frac{dx_5}{dt} &= -\alpha\left(-x_4 + \gamma_{55}x_5 + x_3\right) \\
\frac{dx_6}{dt} &= -\alpha\left(-g\left(x_4\right) + x_6\right) \\
g\left(x\right) &= \begin{cases} 0 & x < b_1 \\ m_1\left(x - b_1\right) & x \geq b_1 \end{cases}
\end{aligned} \tag{1}$$

where $m_1 = 15$, $b_1 = 3$, $\gamma_{11} = \gamma_{44} = 0.02$, $\gamma_{12} = \gamma_{45} = 0.5$, $\gamma_{22} = 0.11$, $\gamma_{41} = 0.5$ and $\gamma_{55} = 0.02$. Equations (1.1) contain a fast system and a slow system. The x_1-x_3 equations describe a chaotic Rossler-like [19] system. The x_4-x_6 equations are a damped nonlinear system coupled to the Rossler system. The frequency band of the damped nonlinear system is determined by the time constant α, which is between 0 and 1. If $\alpha = 0.1$, for example, the frequency band of the x_4-x_6 system is 1/10'th of the frequency band of the Rossler system of the x_1-x_3 equations. The parameter β could also vary between 0 and 1.

The 6-d noise robust system was numerically integrated with a 4'th order Runge-Kutta integration routine with a time step of 0.04 s. Figure 1(a) shows x_2 vs.x_1 for $\alpha =$ 0.01 and $\beta = 1.0$, while 1(b) shows x_5 vs. x_4 for these same parameters. Figure 2(a) is a power spectrum of x_1 , while 2(b) is a power spectrum of x_4 , showing the difference in frequencies.

A synchronous response system matching the drive system of eq. (1.1) was also built. The signal x_2 from eq. (1.1) was used as a drive signal. The response system was described by

$$
\begin{aligned}
x_d &= x_2 + \eta \\
\frac{dy_1}{dt} &= -\left(\gamma_{11} y_1 + \gamma_{12} y_2 + y_3 + \beta y_4\right) \\
\frac{dy_2}{dt} &= -\left(y_1 - \gamma_{22} x_d\right) \\
\frac{dy_3}{dt} &= -\left(g\left(y_1\right) + y_3\right) \\
\frac{dy_4}{dt} &= -\alpha\left(\gamma_{44} y_4 + \gamma_{45} y_5 + y_6 + \gamma_{41}\left|y_1\right|\right) \\
\frac{dy_5}{dt} &= -\alpha\left(-y_4 + \gamma_{55} y_5 + y_3\right) \\
\frac{dy_6}{dt} &= -\alpha\left(-g\left(y_4\right) + y_6\right)
\end{aligned}
\tag{2}
$$

The parameters in eq. (2) were chosen to match the parameters in eq. (1). The term η in eq. (2) was an additive white noise term.

When $\eta = 0$ (o noise), the 6-d response system of eqs. (2) synchronized to the 6-d drive system of eqs. (1) (after an initial transient). Additive noise caused a synchronization error. The error in synchronization δ was measured by calculating the rms value of x_4-y_4 when Gaussian white noise was added to the driving signal x_d .

Figure 3 shows the synchronization error δ as a function of the noise rms amplitude η for 2 different values of α, $\alpha = 0.1$ and $\alpha = 0.01$ (with $\beta = 1$). The noise rms amplitude was normalized by the transmitted signal rms amplitude. While the increase in synchronization error with noise was not linear, it was monotonic. There was no threshold effect as seen in [12, 13]. For the smaller value of α, corresponding to a greater difference in time scales between fast and slow systems, noise caused a smaller synchronization error.

Figure 4 shows the synchronization error δ as a function of the slow time constant α for 2 different values of β, $\beta = 1.0$ and $\beta = 0$. The rms amplitude of the added noise was 4 times the rms amplitude of the driving signal x_2. When $\beta = 1.0$, the synchronization error decreases as the slow time constant α decreases, so in an applied setting, synchronization quality in the presence of noise could be adjusted to an arbitrary precision by adjusting the value of α. The practical result is that adequate synchronization may be maintained for any noise level by properly adjusting the relative time scales of the fast and slow systems. This fact was stated in terms of a bit error rate in [18].

Also shown in Fig. 4 is the synchronization error as a function of α when $\beta = 0$. Not only does the synchronization error not decrease with α, the error actually appears to increase for the lowest values of α. Changing the value of β has destroyed the noise robust property of this chaotic system.

Parameter Variation and Periodic Orbits

In order to understand the origin of the noise robustness, it is useful to find out what changes in the chaotic system as the parameter β is varied. From Fig 1(b), the slow part of this chaotic system looks nearly periodic, so it should be useful to study the long period unstable periodic orbits (UPO's) for this system. The Newton-Raphson method is commonly applied to find UPO's [20].

There is a major numerical problem with finding UPO's with periods on the slow time scale of this system. The largest Lyapunov for this system was 0.14 bits/s, while the long UPO's had periods on the order of 1720 s. By the time one slow orbit has been completed, most of the information about the initial conditions of the system will have been erased by the exponential growth of errors caused by the finite precision of the computer. As a result, when the Newton-Raphson method is applied, the range of initial conditions over which it converges is very small.

Because the separation between slow and fast time scales is large for this system, it is possible to approximately separate the 2-frequency Rossler system into a fast system and a slow system using the quasi-steady-state approximation from singular perturbation theory [21]. We may then apply the Newton-Raphson technique to the slow system only, leading to much better convergence.

.Eq. (2) for the synchronized response system may be rewritten as

$$
\begin{aligned}
\alpha \frac{dy_1}{d\tau} &= -\left(\gamma_{11} y_1 + \gamma_{12} y_2 + y_3 + \beta y_4\right) \\
\alpha \frac{dy_2}{d\tau} &= -\left(y_1 - \gamma_{22} x_d\right) \\
\alpha \frac{dy_3}{d\tau} &= -\left(g\left(y_1\right) + y_3\right) \\
\frac{dy_4}{d\tau} &= -\left(\gamma_{44} y_4 + \gamma_{45} y_5 + y_6 + \gamma_{41} \left|y_1\right|\right) \\
\frac{dy_5}{d\tau} &= -\left(-y_4 + \gamma_{55} y_5 + y_3\right) \\
\frac{dy_6}{d\tau} &= -\left(-g\left(y_4\right) + y_6\right)
\end{aligned}
\tag{3}
$$

where $\tau = \alpha t$ represents a slow time scale. In the approximation $\alpha \to 0$, the y_1-y_3 part of eq. (3) becomes a set of algebraic equations, which may be solved for the variables $\bar{y}_1$, $\bar{y}_2$ and $\bar{y}_3$, the quasi-steady-state approximations. Substituting these values into the slow equations yields

$$
\begin{aligned}
\frac{dy_4}{d\tau} &= -\left(\gamma_{41}\gamma_{22}\left|x_d\right| + \gamma_{44} y_4 + \gamma_{45} y_5 + y_6\right) \\
\frac{dy_5}{d\tau} &= -\left(-b_1\left(y_1\right) m_1\left(y_1\right) - \gamma_{22} m_1\left(y_1\right) x_d - y_4 + \gamma_{55} y_5\right) \\
\frac{dy_6}{d\tau} &= -\left(-g\left(y_4\right) + y_6\right)
\end{aligned}
\tag{4}.
$$

The constants m_1 and b_1 from the function $g(y)$ have been written as functions of y_1 because their presence depends on the value of y_1. Because the function $g(y)$ is piecewise linear, it is not possible to find actual algebraic solutions for y_1, y_2 and y_3, but for the purpose of this paper it does not matter. The approximate relations of eq. (4) will be used only to find a Jacobian for use with the Newton-Raphson method for finding UPO's of the low frequency system, so terms not explicitly dependent on the slow

variables will drop out. In the quasi-steady-state approximation, the Jacobian for the slow system is

$$J = \begin{pmatrix} -\gamma_{44} & \gamma_{45} & -1 \\ 1 & \gamma_{55} & 0 \\ \dfrac{\partial g(y_4)}{\partial y_4} & 0 & -1 \end{pmatrix} \tag{5}$$

In this approximation, the values of the fast variables do not appear in the slow Jacobian. The value of y_4 was determined by numerically integrating the full set of equations (without the quasi-steady-state approximation) in the synchronized state..

Unstable Periodic Orbits

Figure 5 shows a long period UPO extracted from eq. (1) using the Newton-Raphson method. The Jacobian required in the Newton-Raphson method was the slow Jacobian of eq. (5). The time constant parameter α was 0.05, and $\beta = 1.0$. The initial conditions on the algorithm were set to find an orbit for which the slow variables completed one period.

Figure 5(b) shows the UPO for the slow variables. This orbit had a period of 174.92 s, which for the slow variables corresponded to a period 1 orbit. Figure 5(a) shows the fast variables for this same orbit. This was a period 20 UPO for the fast variables, which was because the slow time constant α was 1/20.

There may have been more than one period 1 UPO for the slow system for a given set of parameters, so the following numerical calculations do show some fluctuation. It would have been desirable to follow one distinct UPO as the parameters changed and

calculate its properties, but the poor convergence of the Newton-Raphson algorithm for these long periods made tracking of an individual orbit impossible. Normally, one could track a UPO with parameter changes by finding the initial conditions for a UPO, making a small change in a parameter, and using the previous initial conditions as the starting point for a new UPO search, by for these long orbits, the search failed to converge for parameter changes as small as 0.1%.

Because tracking UPO's was not possible, for each new set of parameters, the equations of motion (eq. (1)) were started with random initial conditions. After initial transients died off, the values of the variables in eq. (1) were used as initial conditions in the UPO search. The approximate UPO period was also estimated from eq. (1) and used as an initial condition. The resulting UPO search converged for about 25% of the initial conditions.

Floquet Multipliers

It was believed that the noise robust properties of the system of eq. (1) were related to the stability of the slow system, so the slow Jacobian of eq. (5) was used to calculate the Floquet multipliers for the slow orbit. Figure 6 shows the Floquet multipliers for the slow orbit as the variable β is changed. For $\beta > 0.68$, the Floquet spectrum consists of 2 purely real values (with magnitude < 1) and one 0 value. This is the same type of Floquet spectrum one would see for a linear oscillator driven at its resonant frequency [22]. Although this orbit for the entire 6-d system is unstable, the slow part of the system by itself does not contain any instabilities, so there are no Floquet multipliers > 1 for the slow part of the orbit.

As β goes from > 0.68 to < 0.68, a bifurcation occurs. The Floquet spectrum now contains one zero value and a complex conjugate pair of values. One would expect to see this type of spectrum for a linear oscillator driven off resonance [22].

The bifurcation seen in the Floquet spectrum for the slow orbit corresponds to a loss of the noise robustness spectrum for this system. Figure 7 shows the synchronization error δ for the response system of eq. (2) as β is varied. The rms value of the added noise in this example was twice the rms value of the driving signal. For $\beta > 0.68$, the synchronization error is small, and is unaffected by changes in β. For $\beta < 0.68$, the synchronization error is larger, and increases as β decreases.

Line Widths

Another way to confirm that the slow part of this Rossler system acts like a resonant system is to measure the width of the largest peak in the power spectrum of the x_4 signal. One way to measure the line width is by measuring the Q factor, the ratio of the center frequency of the main peak in the power spectrum to the width of this peak. The width of the peak is the width for which the power is half of the power at the maximum. A larger Q factor corresponds to a narrower line width, meaning that the low frequency part of the Rossler system acts like a narrowly tuned filter. Figure 8 shows the Q factor as a function of β. Note that the vertical axis in Fig. 8 is logarithmic.

The Q factor undergoes a large increase between β=0.4 and 0.6. Above $\beta = 0.6$, the low frequency part of the Rossler system acts like a narrow band filter- below this point, the low frequency part has a much broader bandwidth. Because the bandwidth of

the low frequency part is so small $\beta > 0.6$, it will not be as strongly affected by additive noise as it will be for $\beta < 0.6$.

The dependence of synchronization error on α, as shown in Fig. (3-4), fits with this narrow band filter picture. The Q factor for a filter is the ratio of center frequency to bandwidth, so if a constant Q is maintained, filter bandwidth will decrease as the center frequency of the filter decreases. The center frequency of the low frequency part of the chaotic system is dependent on the time constant α. As the filter bandwidth decreases, less of the noise will fall within the filter pass band, so the effect of noise on the slow part of the system should decrease.

Neuron Model

It is interesting to ask if the noise robust property of the 2-frequency Rossler system shows up in any other systems. Many neurons display 2-frequency behavior, with a smooth low frequency oscillation combined with a high frequency spiking oscillation. Neurons must operate in a noisy environment, so I would like to see if they use a mechanism for noise robustness that is similar to that used in the 2-frequency Rossler system.

Many neuron models represent homoclinic systems. It has been shown that noise can actually enhance synchronization in homoclinic systems [14, 15]. In the model I use below, it has been shown using mutual information that a type of generalized synchronization exists [23] , and that noise can actually enhance this synchronization. I speculate below on a possible mechanism for this synchronization enhancement.

As a representative neuron model, I use a 4-dimensional version of the Hindmarsh-Rose model, This 4-d model was used by Eguia et al. [23] to study information transmission in coupled neurons. I use this model because the low frequency part is 2 dimensional, so that it is possible to study orbits in the slow part of the system only.

The model is given by

$$\begin{aligned}
\frac{dx(t)}{dt} &= y(t) + 3x(t)^2 - x(t)^3 - z(t) + J_{dc} \\
\frac{dy(t)}{dt} &= 1 - 5x(t)^2 - y(t) - gw(t) \\
\frac{dz(t)}{dt} &= \mu\left[-z(t) + 4\left\{x(t) + h\right\}\right] \\
\frac{dw(t)}{dt} &= \nu\left[-w(t) + 3\left\{y(t) + l\right\}\right]
\end{aligned} \tag{6}$$

where $g = 0.0278$, $h = 1.605$, $l = 1.619$, $\mu = 0.00215$, and $\nu = 0.0009$. J_{dc} will be set to a value between 1 and 4.5. The relation of the variables and parameters to a neuron is described in [23].

The neuron model shows different behaviors as the dc current parameter J_{dc} is changed. For $1 < J_{dc} < 3.25$, there were 2 frequencies present in the x signal, which could be either periodic or chaotic. Figure 9(a) shows the x signal for $J_{dc} = 2.0$. For $J_{dc} \geq 3.25$, only single frequency motion is present, as seen in Fig. 4(b).

Once again I search for long unstable periodic orbits for eq. (6). As with the Rossler system above, the large difference in fast and slow timescales makes it difficult to get the algorithm to find UPO's to converge, so the quasi steady state approximation is used to find an approximate system that contains only the slow variables.

The parameters μ and ν are both << 1, so the quasi steady state approximation may be applied to this neuron model in the same manner that it was applied to the Rossler system. Using ν as the small parameter, eq. (6) becomes

$$\begin{aligned}
\nu\frac{dx(t)}{d\tau} &= y(t) + 3x(t)^2 - x(t)^3 - z(t) + J_{dc} \\
\nu\frac{dy(t)}{d\tau} &= 1 - 5x(t)^2 - y(t) - gw(t) \\
\frac{dz(t)}{d\tau} &= \frac{\mu}{\nu}\left[-z(t) + 4\{x(t) + h\}\right] \\
\frac{dw(t)}{d\tau} &= \left[-w(t) + 3\{y(t) + l\}\right]
\end{aligned} \tag{7}$$

Taking the limit in which ν and μ become small, the left hand side of the *x* and *y* equations can be set to zero, and the resulting equations may be solved for the quasi steady state approximations to *x* and *y*.

Solving for the quasi steady state values of *x* and *y* gives 3 roots, but 2 of these roots are complex, so only the real root is used. The steady state values are substituted into the *z* and *w* equations, which may then be used to find a Jacobian for the slow system. This slow Jacobian is used with the Newton-Raphson method to find slow UPO's, and the slow Jacobian is also used to find Floquet multipliers for these slow UPO's. No slow UPO's were found for $J_{dc} \geq 3.25$. Above this value of J_{dc} , all the variables in the neuron simulation are in the same frequency band.

Figure 10 shows a typical UPO for the neuron model, for a dc current of $J_{dc} = 2.7$. Fig. 10(a) shows the fast variables *x* and *y* , while 10(b) shows the slow variables *z* and *w*. The Floquet multipliers for the low frequency UPO's were all real and < 1.

Noise Robustness in the Neuron Model

Eguia et al do consider the effect of added noise on information transmission on their model neuron. They couple 2 of these neurons through a model of a synapse, and drive the first neuron with a series of pulses. They use the mutual information between the pulse signal and the x signal from each neuron, or between the x signals from the 2 neurons, as a measure of information transmission. In one experiment, both neurons have $J_{dc} = 3.4$, in the single frequency region. They find that when noise is added to the pulse signal, the mutual information between the pulse signal and either neuron goes through a maximum as the noise level is increased. Adding noise in some cases aids in information transmission.

One possible cause for this increase in information transmission is the presence of quadratic nonlinearities in the neuron model. The quadratic nonlinearities operating on the added noise will cause a DC offset which changes the effective value of J_{dc} . When Gaussian white noise with an rms value of 0.1 is added to the equation for dx/dt, with $J_{dc} = 3.4$, the resulting x signal actually has 2 frequencies, as it would for a lower value of J_{dc} . Applying the Newton-Raphson algorithm to the noise driven neuron model, it is actually possible to find long UPO's for $J_{dc} = 3.4$ and a noise amplitude of 0.1. Figure 11 shows one of these UPO's, which has all real Floquet multipliers < 1. The added noise shifts the neuron model into the 2-frequency region, and, as shown in the Rossler example above, when the slow part of the system has UPO's with real Floquet multipliers, the system is robust to added noise.

As demonstrated in [23], there is a threshold above which this added noise no longer enhances synchronization. Noise enhanced synchronization with a threshold was

also seen in homoclinic chaos in a laser in [14, 15]. In both the neuron model and the laser studies, noise altered the time scales of the chaotic system, resulting in enhanced synchronization.

Conclusions

It has been shown that when a 2 time scale system is properly structured, the low frequency part of the system can act like a resonant system, so that the low frequency dynamics is not greatly affected by added noise. Computing dynamical quantities, such as Floquet multipliers, for a two frequency system can be difficult because the low frequency dynamics evolves on a time scale that is long compared to the largest Lyapunov exponent for the chaotic system. In order to make calculations easier, the quasi steady state approximation from singular perturbation theory was used to separate the entire dynamical system into independent fast and slow systems.

Numerical comparisons to a model of a neuron show that the low frequency dynamics of the neuron model also resembled a resonant system. Two frequency dynamics is known to exist in real neurons, so it is possible that the mechanisms for noise robustness described here also exist in real neurons.

References

[1]L. M. Pecora and T. L. Carroll, Physical Review Letters **64**, 821 (1990).
[2]L. O. Chua, T. Yang, G.-Q. Zhong, et al., IEEE Transactions on Circuits and Systems Part I **43**, 862 (1996).
[3]K. M. Cuomo, A. V. Oppenheim, and S. H. Strogatz, IEEE Transactions on Circuits and Systems Part II **40**, 626 (1993).
[4]L. Kocarev and U. Parlitz, Physical Review letters **74**, 5028 (1995).
[5]G. Kolumban, M. P. Kennedy, and L. O. Chua, IEEE Transactions on Circuits and Systems-Part I: Fundamental Theory and Applications **44**, 927 (1997).
[6]K. Murali and M. Lakshmanan, Physical Review E **48**, 1624 (1993).
[7]A. V. Oppenheim, K. M. Cuomo, R. J. Barron, et al., in *3rd Technical Confrence on Nonlinear Dynamics and Full Spectrum Processing*, edited by R. A. Katz (AIP Press, Mystic, CT, 1995).
[8]U. Parlitz, L. Kocarev, T. Stojanovski, et al., Physical Review E **53**, 4351 (1996).
[9]N. F. Rulkov and L. Tsimring, International Journal of Circuit Theory and Applications **27**, 555 (1999).
[10]C. Williams, IEEE Transactions on Circuits and Systems Part I: Fundamental Theory and Applications **48**, 1394 (2001).
[11]A. Abel, W. Schwartz, and M. Goetz, IEEE Transactions on Circuits and Systems Part I **47**, 1726 (2000).
[12]C. Zhou and J. Kurths, Physical Review Letters **88**, 230602 (2002).
[13]C. Zhou, J. Kurths, I. Z. Kiss, et al., Physical Review Letters **89**, 014101 (2002).
[14]C. S. Zhou, J. Kurths, E. Allaria, et al., Physical Review E **67**, 015205(R) (2003).
[15]C. S. Zhou, J. Kurths, E. Allaria, et al., Physical Review E **67**, 066220 (2003).
[16]S. Boccaletti, J. Kurths, G. Osipov, et al., Physics Reports **366**, 1 (2002).
[17]T. L. Carroll, Physical Review E **64**, 015201(R) (2001).
[18]T. L. Carroll, IEEE Transactions on Circuits and Systems Part I: Fundamental Theory and Applications **48**, 1519 (2001).
[19]O. E. Rossler, Z. Naturforsch. **38a**, 788 (1983).
[20]T. S. Parker and L. O. Chua, *Practical Numerical Algorithms for Chaotic Systems* (Springer-Verlag, New York, 1989).
[21]P. Kokotovic, H. Khalil, and J. O'Reilly, *Singular Perturbation Methods in Control: Analysis and Design* (SIAM, Philadelphia, 1999).
[22]J. Guckenheimer and P. Holmes, *Nonlinear Oscillations, Dynamical Systems, and Bifurcations of Vector Fields* (Springer-Verlag, New York, 1990).
[23]M. C. Eguia, M. I. Rabinovich, and H. D. I. Abarbanel, Physical Review E **62**, 7111 (2000).

Figures

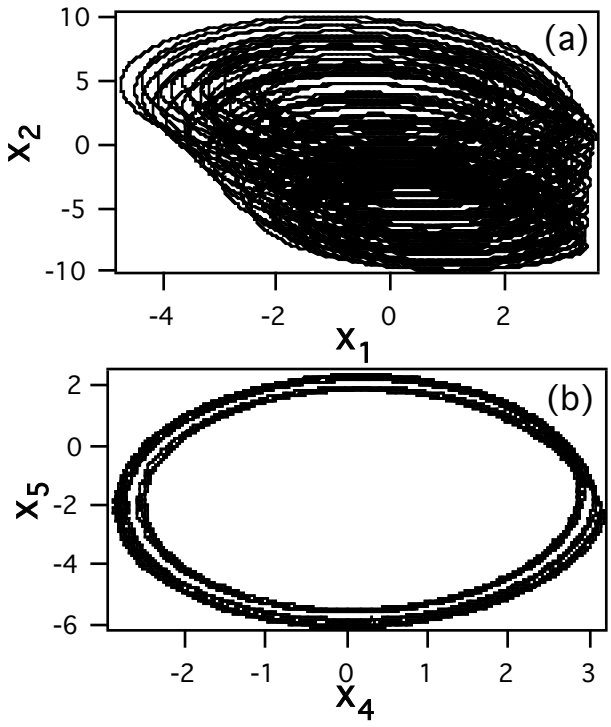

Figure 1. Attractors for eq. (1)

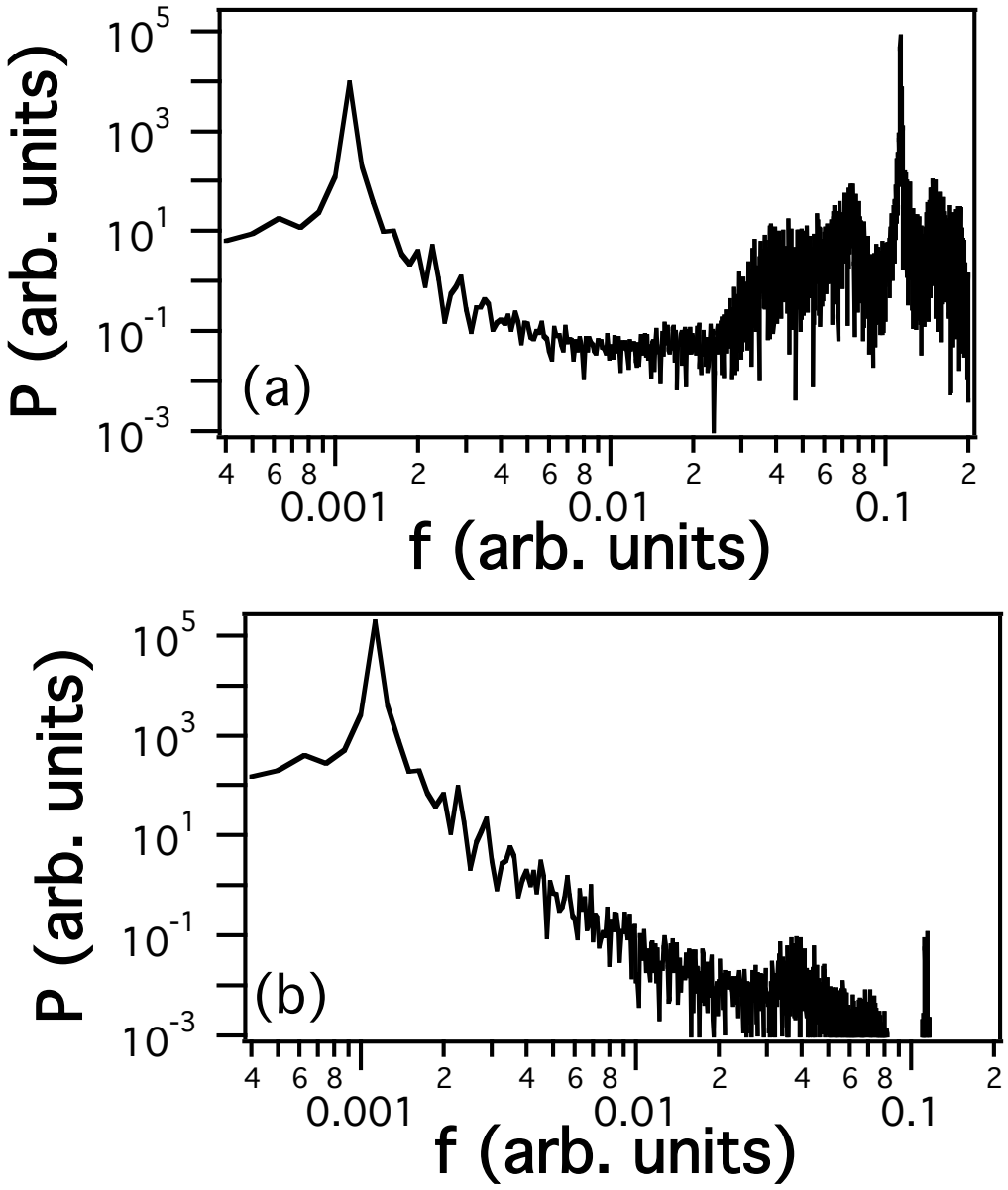

Figure 2. (a) Power spectrum of x_1 (peak frequency = 0.113). (b) Power spectrum of x_4 (peak frequency = 0.00113).

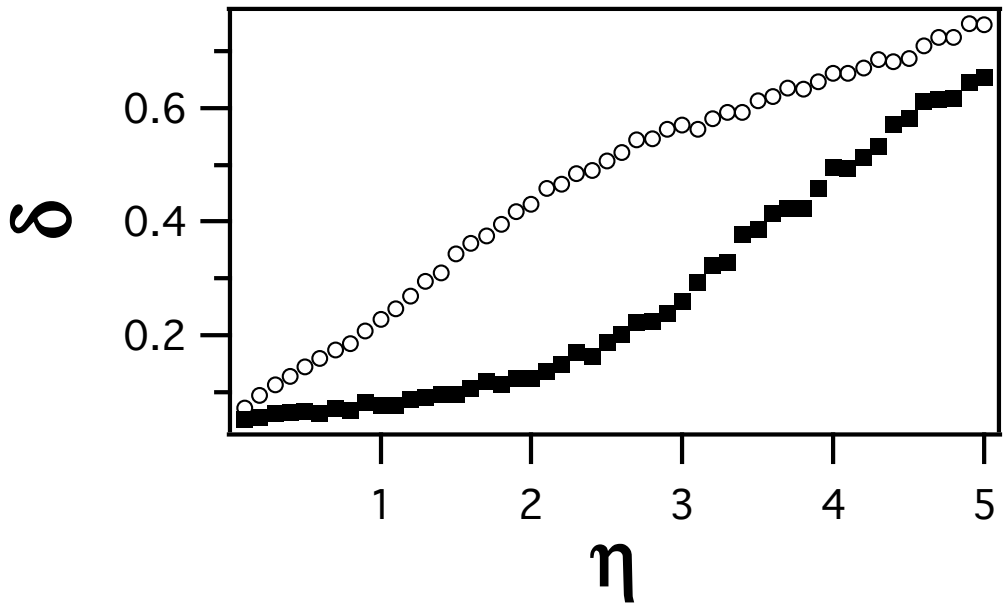

Figure 3. Synchronization error δ as a function of normalized noise rms amplitude η for slow time constant $\alpha = 0.1$ (open circles) or 0.01 (filled in squares).

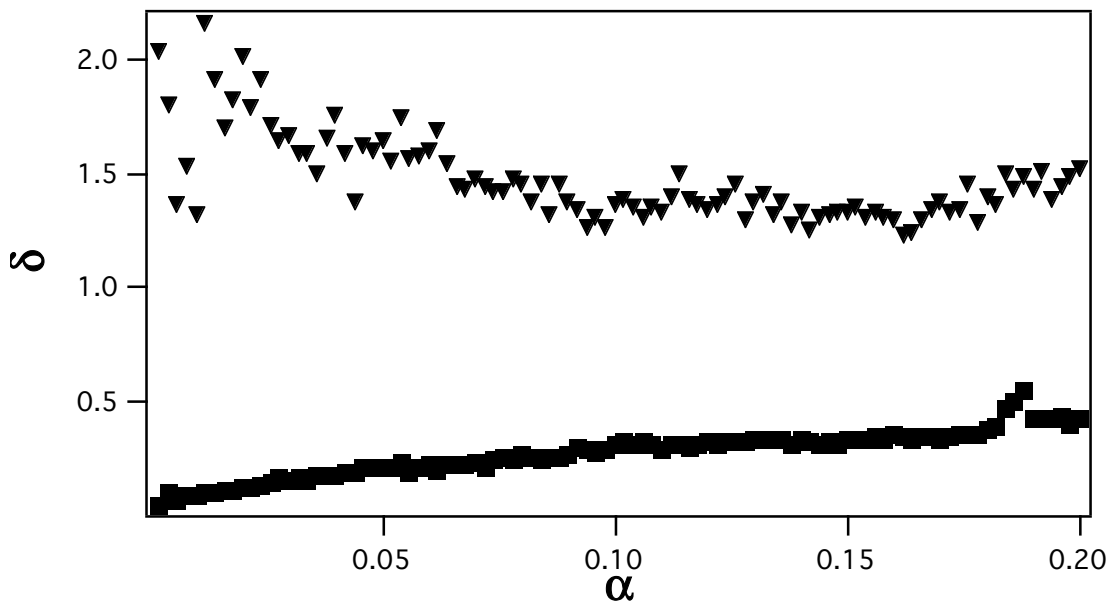

Figure 4. Sync error δ as a function of slow time constant α. The squares are for β = 1.0, while the triangles are for β = 0.0.

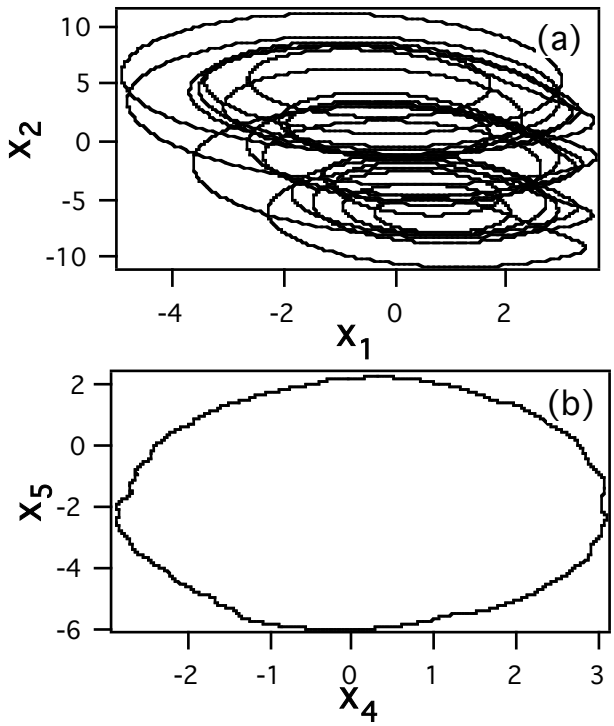

Figure 5. An unstable periodic orbit for the chaotic system of eq. (1).

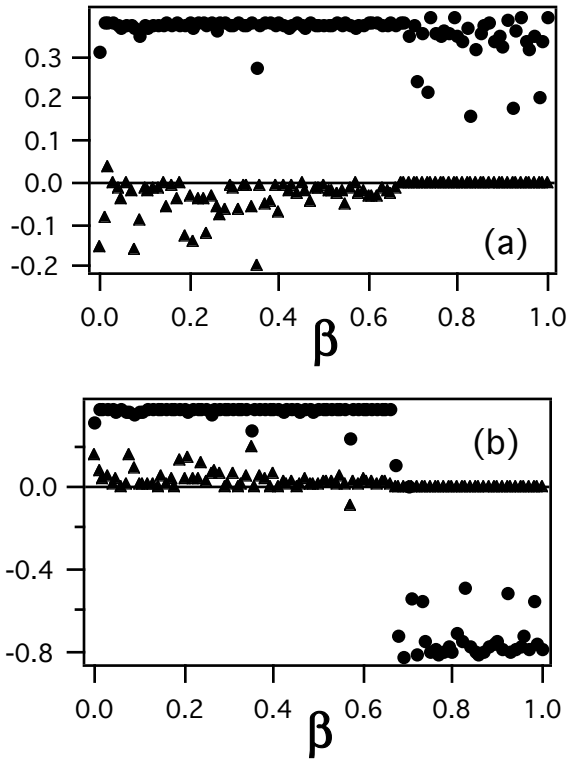

Figure 6 (a) and (b) are the nonzero Floquet multipliers for the slow UPO as β is changed. The circles are the real parts of the Floquet multipliers, while the triangles are the imaginary parts. There is a bifurcation at $\beta = 0.68$.

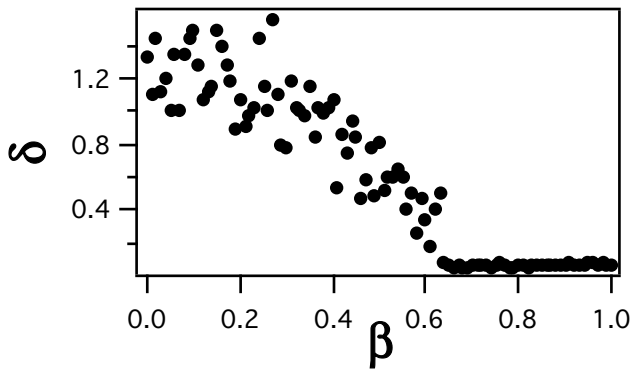

Figure 7. Synchronization error δ as a function of β. The rms amplitude of the added Gaussian white noise is twice the rms amplitude of the driving signal. The noise robustness property appears to be lost for $\beta < 0.68$, corresponding to the bifurcation in the Floquet spectrum.

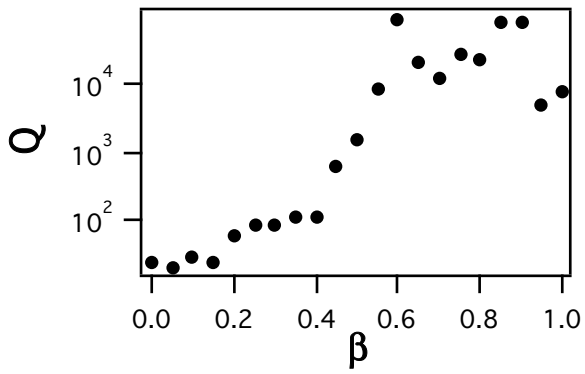

Figure 8. *Q* factor for the low frequency part of the Rossler system as a function of β. Note that the vertical axis is logarithmic.

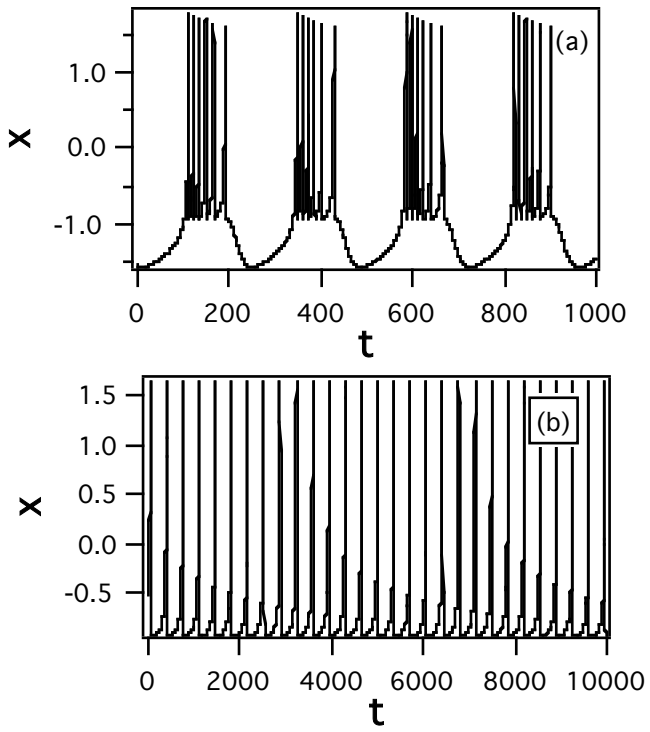

Figure 9. (a) *x* signal for J_{dc} = 2.0. Note that there are 2 frequencies present. (b) *x* signal for J_{dc} = 3.4. Only 1 frequency is present.

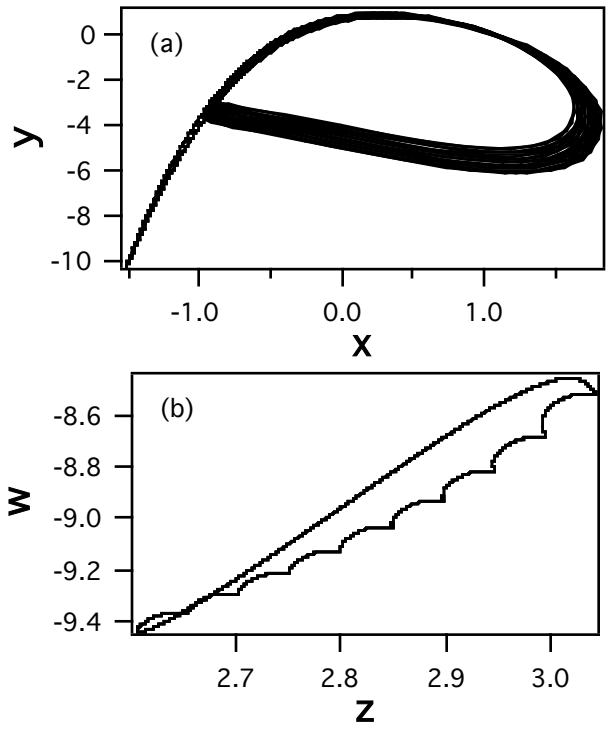

Figure 10. Typical slow UPO for the neuron equations, for J_{dc} = 2.7. (a) shows the fast variables *x* and *y*, while (b) shows the slow variables *z* and *w*.

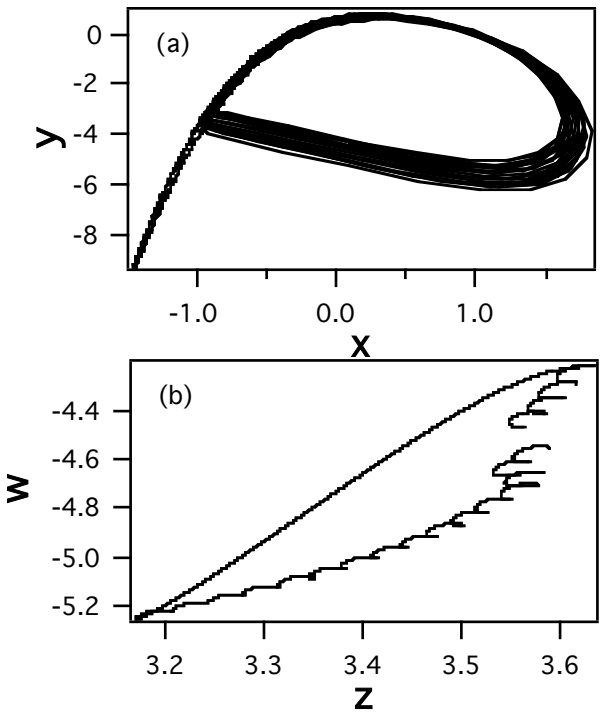

Figure 11. UPO seen in the neuron model when J_{dc} = 3.4 (single frequency region), but noise with an amplitude of 0.1 was added. (a) shows the fast variables, and (b) shows the slow variables. Compare this figure to fig. 10.